# Further Optimization of Solar Electronic Yarns for Developing Large, Stretchable Knitted Textile Solar Panels


Parvin Ebrahimi
*Nottingham School of Art & Design*
*Nottingham Trent University*
*Nottingham, United Kingdom*
*parvin.ebrahimi2022@my.ntu.ac.uk*

Arash Moghadassian Shahidi
*Nottingham School of Art & Design*
*Nottingham Trent University*
*Nottingham, United Kingdom*
*arash.shahidi@ntu.ac.uk*

Demosthenes Koutsogeorgis
*School of Science & Technology*
*Nottingham Trent University*
*Nottingham, United Kingdom*
*demosthenes.koutsogeorgis@ntu.ac.uk*

Carlos Oliveira
*Nottingham School of Art & Design*
*Nottingham Trent University*
*Nottingham, United Kingdom*
*jose.oliveira@ntu.ac.uk*

Jake Kaner
*Nottingham School of Art & Design*
*Nottingham Trent University*
*Nottingham, United Kingdom*
*jake.kaner@ntu.ac.uk*

Tilak Dias
*Nottingham School of Art & Design*
*Nottingham Trent University*
*Nottingham, United Kingdom*
*tilak.dias@ntu.ac.uk*

Theo Hughes-Riley
*Nottingham School of Art & Design*
*Nottingham Trent University*
*Nottingham, United Kingdom*
*theo.hughes-riley@ntu.ac.uk*



***Abstract*—Energy harvesting methodologies provide an efficient solution for powering portable and wearable electronic devices, with solar energy being one of the most promising sources. Solar energy harvesting stands out as it offers a significant power density, making it a highly effective alternative to traditional batteries. Integrating solar energy technology into textiles has several advantages, including improving the efficiency of wearable devices and enhancing the system's sustainability. This study advances prior research on incorporating solar cells into electronic yarns to create solar textile. A solar electronic yarn sees miniature solar cells soldered onto thin Litz wires in parallel, components encapsulated within a discrete, resin micro-pod, and finally, the cells and wires are covered in a textile braid. This work explores improving current solar E-yarns and their textile integration. The current research presents a significant step in optimising the mold used for the encapsulation process. This research details these improvements, demonstrating their impact on the overall performance and efficiency of the system. Finally, with these improvements, a prototype knitted solar textile, which is foldable, drapeable, breathable, and stretchable was crafted and underwent testing under direct sunlight.**



***Keywords—energy harvesting; photovoltaic; electronic yarn; electronic textiles; solar textile.***


## I. INTRODUCTION

Advances in technology have made electronic components smaller and more power-efficient. The improvements in the size and shape of these components have led to microscale devices significantly reducing their power requirements to the milliwatt and microwatt range. This has allowed devices like wearable and mobile devices [1], sports and wellness [2], medical and health monitoring [3], military [4], [5], consumer electronics [6], entertainment [7], fashion wear [8], and communications [9] to run on minimal battery power.

Energy availability is a significant challenge for many mobile or wearable applications as they normally run on rechargeable batteries. However, batteries' reliability, environmental impact at disposal, lifetime operation, bulkiness, and rigidity are challenges. As a result, researchers are trying to totally or partially eliminate the use of batteries for wearable electronic devices.

This has driven research into energy harvesting, which means capturing power from ambient sources to support low-power electronic devices [10]. Ambient energy sources, such as kinetic energy (wind energy, wave energy, human motion, mechanical vibration), electromagnetic energy (photovoltaic, radio-frequency), thermal energy (thermoelectric generators, solar-thermal, geothermal gradients of temperature), atomic energy (nuclear, radioactive decay), biological energy (biofuels, biomass), piezoelectric energy (pressure and strain), or hydraulic energy (hydropower) are central to ongoing research aimed at developing sustainable energy solutions [11], [12], [13], [14], [15]. These technologies capture energy from ambient environmental sources, offering a way to power devices with minimal environmental impact and reducing reliance on traditional batteries.

Table 1 provides an overview of the most common energy harvesting methods currently used, highlighting their power densities and limitations. Solar energy harvesting emerges as the most efficient, offering significantly higher power density than alternatives like kinetic or thermal methods. However, each technique has its advantages depending on specific conditions and applications, and making them suitable for different uses despite their limitations is challenging [16], [17].

TABLE I. COMPARISON OF THE POWER BETWEEN VARIOUS ENERGY HARVESTING TECHNIQUES.

| Type | Power density ($W/cm^2$) reported in [16] | Power density ($W/cm^2$) reported in [17] | Limitations |
|---|---|---|---|
| Solar | $2\times10^{-5}$-0.2 | $1.5\times10^{-3}$ | Light intensity |
| Thermal | $3\times10^{-3}$-0.03 | $4\times10^{-5}$ | Thermal difference |
| RF wave | $2\times10^{-10}$- $1\times10^{-3}$ | 0.02 | Distance and RF harmonic |
| Vibration/ piezoelectric | $4\times10^{-6}$-$2\times10^{-4}$ | $5\times10^{-4}$ | Vibration frequency |
| Vibration/ electromagnetic | $2.5\times10^{-7}$-0.01 | $4\times10^{-6}$ | AC/DC conversion |

Energy harvesting is creatively combined across various industries to enhance efficiency and sustainability. With intuitive design, wearable technology now features energy-harvesting textiles, enabling smart clothing to generate power from body heat, movements, and environmental factors [9].

Textiles are an excellent medium for integrating low-power electronics, serving as effective platforms for capturing and storing various forms of energy. Their large surface area allows for significant interaction with the human body and the surrounding environment, making energy harvesting more efficient. The term "electronic textiles" or "E-textiles", describes fabrics incorporating electronic components, that can enable them to sense and respond to changes in their surroundings. This integration opens up exciting possibilities for smart clothing and wearable technology [18], [19]. Consequently, textile-based energy harvesting, in which electronic components are integrated within the textile, has gained a growing interest over the last few decades [20], [21], [22], [23], [24], [25], [26].

Several methods exist for integrating electronics into fabrics. The first generation of E-textiles mainly appeared in laboratories or as specially made clothing and did not resemble regular garments. Electronic devices were typically simply attached to the fabric surface, such as through lamination. In the second generation, conductive yarns were knitted or woven into the textile structure to make it electronically functional, however, this technique could only lead to certain types of devices. To address this, researchers developed a third generation of electronic textiles, where integrated components or circuits were fully embedded into the yarn before the fabric or garment was made, representing a significant advancement [27], [28]. This work focuses on E-yarn or “electronic yarn” technology which involves embedding microelectronic components, directly into the structure of yarns before they are woven or knitted into fabrics. This innovation allows textiles to have electronic functionality while maintaining traditional fabrics' look, feel, and flexibility. Unlike earlier wearable technologies that attached devices externally, E-yarn integrates these components seamlessly, making the electronics nearly invisible and more durable for a variety of applications, such as health monitoring, smart clothing, or responsive textiles [29], [30].

This study centres on integrating solar energy harvesting into textiles namely Solar Textiles (fabrics embedded with solar cells or photovoltaic materials, enabling them to capture sunlight and convert it into electricity) using E-yarn technology. This innovative technology integrates miniature PV cells into textiles, allowing clothing or any other textile structures like tents, curtains, flags, umbrellas, caravans, car shades, or sails to harness solar energy and turn it into electric power. This technology opens up the possibility for a wide array of applications by significantly reducing the reliance on conventional batteries, ultimately enhancing their longevity and efficiency. It acts as a supplementary power source for devices such as wearables and health monitoring gadgets.

Building on prior research on the creation of solar E-yarns [21], [31], [32], this study introduces advancements and describes challenges in creating encapsulation molds, to encapsulate the solar cells and solder joints with a small structure, namely a micro-pod, to secure the solar cells from mechanical and chemical stresses. The work also investigates the base structure for making knitted solar textiles. Finally, with these improvements, a prototype, knitted solar textile, which is foldable, drapeable, and stretchable was crafted and tested in an outdoor environment.

## II. MATERIALS AND METHODS

### A. Solar electronic yarn production

The production of the solar E-yarn starts by soldering miniature solar cells onto fine conductive wires. The stages include: (a) establishing interconnections between solar cells (5 × 2 × 0.2 mm; unbranded polycrystalline silicon solar cells, commercially sourced) and Litz wires (Type 1 Litz, Osco Limited, Milton Keynes, Buckinghamshire, United Kingdom; see Fig. 1.a); (b) encapsulation of the component within a polymer micro-pod (DYMAX, Multi-Cure® Adhesive & Coating, 9001-E-V3.5, Torrington, Connecticut, USA) along with two high tensile strength supporting yarns (VECTRAN™, Kuraray America, Inc., Houston, TX, USA) to improve the mechanical strength of the connections and to stabilise the components during the braiding process (c). Covering the components with a braided outer layer (Fig. 1) [32].

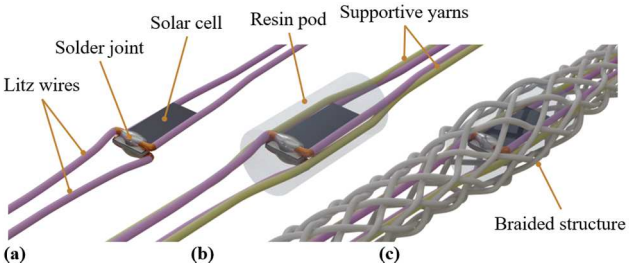


Fig. 1. Stages of making solar E-yarn; a. soldered, b. encapsulated c. braided.

### B. Encapsulation mold development

One of the challenges of making solar textiles was to orientate the solar E-yarns with the photoactive area facing upwards (toward the light source) within the textile. To ensure solar photovoltaic cells are upward-facing when integrated into woven or knitted structures different encapsulation molds were designed and tested. By considering manufacturing feasibility, compatibility with fabric structures, and the objective of avoiding sample rotation during weaving or knitting, the micro-pod shapes were designed with a flat-edge, including various semi-cylindrical shapes. A semi-cylindrical shape for the mold (and therefore micro-pod) is ideal as on one side it had a shape like a yarn, which is typically cylindrical, and at the same time it had a flat surface to guide the yarn positioning,

ensuring that when the solar E-yarn is inserted into the fabric, the front surface remained easily identifiable.

Various methods and techniques were tested to make the semi-cylindrical mold, using a two-part mold and a single-part mold.

The split mold, or two-part mold, with a core and cavity, was designed using SolidWorks (SolidWorks, version 2023, Dassault Systèmes, Waltham, MA, USA). Then it was 3D printed using a resin 3D printer by stereolithography (SLA) technology (Form 3+ Resin 3D Printer, Formlabs, Somerville, MA, USA) to create a physical model of the object called the master model from which the mold could be cast. After preparing the master model, to create the mold, the master model was placed in a container, and silicone (Polytek Dev' Corp®. PlatSil®Gel-OO & Gel-10 Soft, Translucent, RTV Liquid Silicone Rubbers for Theatrical Prosthetics, Lifecasting & Mold Making Applications. Technical Bulletin, Easton, PA, USA) was poured over it, after curing the silicone (approximately ~ 3-4 hours), the mold was created (Fig. 2).

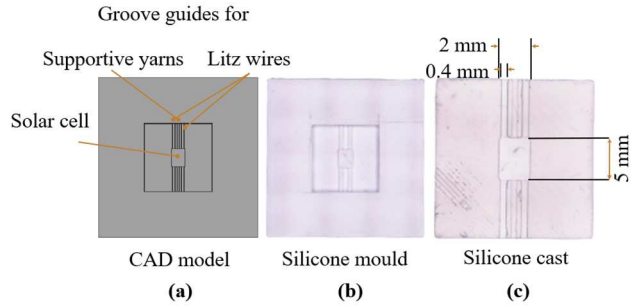


Fig. 2. Stages of creating the mold using a two-part master mold. (a) Designing the CAD model in software. (b) 3D printing the master mode. (c) Casting the mold with silicone.

To design a single-part mold, different 3D printing methods and materials were evaluated to produce the optimal master mold. The three most established types of 3D printers for plastic parts are namely stereolithography (SLA), selective laser sintering (SLS), and fused deposition modeling (FDM). In our investigation, we examined two printers, FDM and SLA. For the FDM printer (Construct 1 3D Printer, Construct3D, 2023, Lincoln, UK) two materials: PLA (polylactic acid filament; ePLA-Lite 3D Printer Filament, eSUN; Shenzhen, China; Fig. 3a), and PVA (Polyvinyl Alcohol; PS-PVAP-175-0500-NA, PrimaSelect, PrimaCreator; Malmö, Sweeden; Fig. 3c) were tested. Also, for SLA technology we used (Form 3+ Resin 3D Printer; Formlabs, Somerville, MA, USA) with resin (rigid 20K resin; Formlabs, Somerville, MA, USA; Fig. 3b).

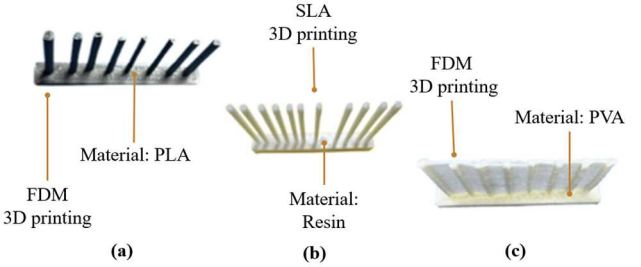


Fig. 3. Master molds created to produce a single-part encapsulation, with the same CAD mode. Each column measures 3mm in width and 50 mm in length. (a) Fused Deposition Modeling of polylactic acid filament which larger layer lines. (b) Stereolithography of rigid 20K resin with finer layer lines. (c) Fused Deposition Modeling of Polyvinyl Alcohol with a temprorary scaffold between layers that is soluable in water.

### *C. Solar Textile construction*

To identify the most suitable base material for embedding solar E-yarns into textiles, various materials and structures were evaluated. In contrast to the previous work where the panel was conducted as a woven fabric using Polyester as the primary material (either a single cloth [33] or double cloth structure by [31]). This work explored creating a knitted solar textile because of the intrinsic superior stretchability and breathability of knitted structures. Unlike woven fabrics, which are more rigid and structured, knitted fabrics are naturally stretchable due to their looped construction, offering greater flexibility and adaptability, especially for wearable applications. Another key factor in our choice was sustainability. Throughout the knitted fabric, channels can be created that enable the efficient integration and removal of solar electronic yarns, either at the end of the product's lifecycle or to facilitate repairs in the case of breakage or faults via these channels, which would be much harder to achieve with a woven structure.

To do so, different arrangements, structures, and materials were explored to find the optimum way to insert the solar E-yarn inside the fabric. An initial textile sample was produced using polyester yarn (1/167/48, J. H. Ashworth & Son Ltd., Hyde, United Kingdom) with a plain interlock (all needles) structure on a flat-bed knitting machine (Stoll CMS ADF 32 W E7.2; Reutlingen, Germany).

A second sample was produced incorporating five channels, each containing one solar E-yarn connected in parallel. The solar E-yarns were connected in parallel to optimise the overall electrical performance of the system. Within each solar E-yarn, two polycrystalline solar cells (dimensions 2×5 mm, unbranded polycrystalline silicon solar cell, commercially sourced) were embedded and connected in parallel, ensuring that both the individual yarns and the solar cells contributed effectively to the power generation. The E-yarn used a tubular mold (i.d. = 3 mm, length = 7 mm; silicone) for encapsulation. The mold was filled with an ultra-violet (UV) curable Acylated Urethane resin (Dymax 9001-E-V3.5; Dymax Corporation, Torrington, CT, USA) and cured using a UV source (Dymax BlueWave® QX4™; Dymax Corporation, Torrington, CT, USA). Then a fibrous sheath around the micro pod was made by using 12 multi-twisted transparent filaments (Nm 1/80 SUKERU #DT-10, Material Composition: 70% Nylon, 30% Polyester; Winning Textile Ltd, Kwun Tong, Hong Kong) through the use of a suture braiding machine (RU1/24-80; Herzog GmbH, Oldenburg, Germany).

The final panel (the knitted solar textile) with the dimensions of 180 × 140 mm, and an active area of 100 ×1 00 mm featured a total of six knitted channels, the width of the channel was 5 mm which was designed for six solar E-yarns to be placed. Each solar E-yarn was composed of eight solar cells, each measuring 2 × 5 mm. These cells were created by cutting larger Mono-Crystalline Bifacial PERC solar cells (dimensions of 157×157 mm, 21.7% efficiency, 5.3 watts/cell; ALLMEJORES, Dongguan, China). Then the nylon insulator layer and enamel of the Litz wires (Type 1 Litz, Osco Limited, Milton Keynes, Buckinghamshire, United Kingdom) were removed using a soldering iron (Antex XS25; Antex Electronics Limited, Plymouth, UK) which had a small

amount of lead-free solder applied to them (diameter = 1.27 mm; comprising tin, natural rosin, silver, and copper; SA305; RS Components Ltd., Corby, UK). After connecting these eight solar cells in parallel, two supportive multistrand yarns (VECTRAN™, Kuraray America, Inc., Houston, TX, USA) were pre-encapsulated alongside the Litz wires. Then they were fed into a discrete tubular mold (i.d. = 3 mm, length = 7 mm; silicone), and were filled with a UV curable Acrylated Urethane resin (Dymax 9001-E-V3.5) and cured using a UV source (Dymax BlueWave® QX4) for 50 seconds. A fibrous sheath containing 24 multi-twisted transparent filaments (Nm 1/80 SUKERU #DT-10, Material Composition: 70% Nylon, 30% Polyester; Winning Textile Ltd, Kwun Tong, Hong Kong) was made around the ensemble using a suture braiding machine (RU1/24-80) to create the solar E-yarns. These yarns were them inserted into each channel and this arrangement resulted in a cumulative total of 48 solar cells integrated into the swatch. In terms of connectivity, the configuration included three solar E-yarns positioned at the top, which are connected in series with one another. Similarly, three solar E-yarns located at the bottom were also connected in series. This arrangement let the top and bottom groups connect in parallel, which created positive and negative electrical connections for the swatch. By utilising this series-parallel configuration, the design optimised both the voltage and current output from the solar cells, enhancing the overall efficiency of the solar energy harvesting system, and making fault detection or degradation identification easier.

### *D. Solar electronic yarn and solar textile testing*

Solar E-yarns in this work were tested using a solar simulator (LSH-7320 ABA LED solar simulator; Newport Corporation, Stratford, USA) at 1 sun illumination (1000 W/m$^2$ and 25°C standard cell temperature). The electrical characterisation of the solar E-yarns was conducted using the Keithley Parameter Analyzer (Keithley 4200A-SCS Parameter Analyzer; Tektronix Inc., Beaverton, Oregon, USA) to extract the important data including the maximum power point ($P_{max}$), the short circuit current ($I_{sc}$), and the open circuit voltage ($V_{oc}$).

An outdoor testing setup was established using a solar power meter (MP780966 Solar Power Meter; Multicorp Pro., Shanghai, China), a Keithley analyser, a calibrated reference cell (SCI-REF-Q, Solar Reference Cell; Sciencetech, Ontario, Canada), and the swatch. An experimental station with an adjustable angle was mounted on the setup to capture maximum sunlight, allowing it to be angled for optimal sun exposure based on the sunlight meter readings. A calibrated reference cell was also positioned to accurately measure the sunlight intensity, which was then converted to a standard reference of 1 Sun. The electric output from the solar textile was measured using the Keithley Parameter Analyzer (see Fig. 4).


Fig. 4. Experimental setup for the outside testing.

### *E. Textile properties testing*

To evaluate the textile features of the swatch, both air permeability and tensile testing were conducted. Air permeability refers to the ability of a material to allow air to pass through it. It is essential because it gauges how well the fabric allows air to flow through, directly influencing comfort and breathability. The experimentation followed the approach outlined in ASTM D737 (Standard Test Method for measuring the air permeability of textile fabrics). It determines the rate at which air passes through a fabric under a specified air pressure difference between two surfaces of the material, which gives the fabric porosity and breathability. The investigation was conducted using the AirPro air permeability tester (James H. Heal & Co., Ltd., Halifax, UK). The tests were carried out on a 20 cm$^2$ circular area (as specified in the standard) targeting a 125 Pa pressure, similar to tests conducted by others in the literature for conventional textiles [34]. The sample was clamped and checked for wrinkles or deformations both before and after inserting the solar E-yarns into the fabric (Fig. 5). This was repeated five times.

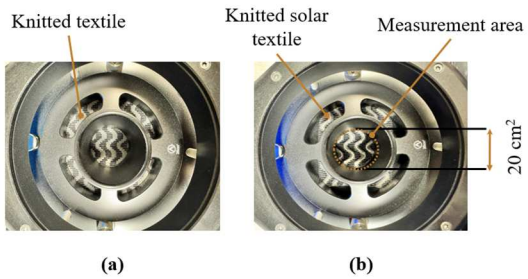


Fig. 5. Images of the swatch placed within the air permeability testing system, a. before and b. after inserting solar E-yarns inside of the fabric.

Stretchability is another crucial property of textiles, especially for applications in wearable and performance fabrics where comfort is essential. To evaluate how much a textile can stretch and tolerate deformation, several standardised tests can be conducted, such as tensile testing. In tensile testing, the sample is placed and held using pneumatic grips to avoid any slippage and gradually stretched (in this case 50 mm/min) while measuring the applied force and strain until the fabric reaches the desired strain, which in this study was 25 %and 12 % respectively. Key parameters measured include the strain percentage and the force required to gain the desired strain. The tensile testing was conducted using a zwickiLine Z2.5 TN+ Material Testing Machine (ZwickRoell GmbH&Co.KG, Ulm, Germany). The test was constructed in both knitted fabric structural directions; the course (horizontal) and wale (vertical) directions, to evaluate the stretchability across the fabric. An experimental setup was developed to examine how the electrical properties (current) of the swatch change under applied force. An 85 W daylight-balanced lamp (Spare 85W 5500K CFL Bulb; FOTGA, Shenzhen, China) was used to focus the light. A cover was created around the lamp with a square opening measuring 50 × 50 mm at the end, which allowed the light to be concentrated on the centre of the swatch. This setup served as the light source to observe the changes and was positioned close to the surface of the swatch. A digital multimeter (Truevolt 34461A Bench Digital Multimeter; Keysight Technologies, Santa Rosa, California, U.S.) was connected to the positive and negative terminals of the swatch to record electrical data continuously. At the same time, the sample was subjected to stretching force.

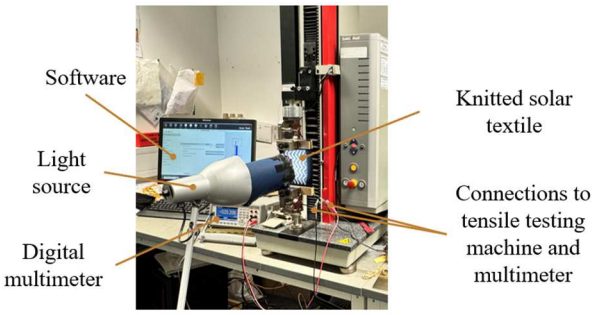


Fig. 6. Set up for tensile testing to assess the electrical response of the solar textile fabric during two stretching modes: course direction and wale direction.

## III. Results

### A. Encapsulation modification and characterization

Initially, the two-part mold was trialed. This mold design was not suitable for encapsulating solar cells because, during encapsulation with Dymax 9001 UV-curable resin, the resin would flow into the grooves of the Litz wires and Vectran™ supporting yarns. Due to capillary flow, or the unintended movement of resin into areas where it was not desired, the final mold's micro-pod shape and curing process did not maintain the intended form (see Fig. 7). This deformation was particularly challenging to overcome, as while capillary flow can be somewhat controlled by material modification and design adjustment, it cannot be fully eliminated since this is a small scale mold (2 to 5 mm), and resin tends to flow into the groves and lines. On the other hand, this deformation impacts light transmission, causing light scattering and reducing electrical performance, and from a design standpoint it also disrupts the visual consistency of the micro-pod. To address this issue effectively, a one-part mold may be preferable to minimize unwanted resin flow and improve overall encapsulation precision.

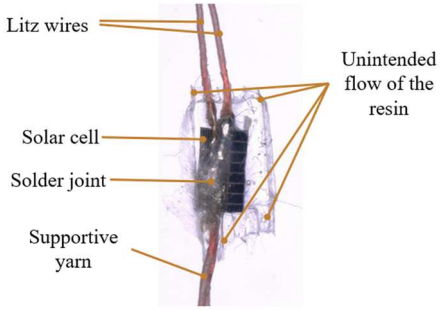


Fig. 7. Example micro-scope image of a soldered solar cell encapsulated within a resin micro-pod with a flat edge (dimensions 2×5 mm). The encapsulation was achieved with a two-part mold; the capillary flow of resin in grooves led to the deformation of the final shape.

Encapsulation with a single-part mold was then examined. Three types of molds were evaluated, this evaluation examined the visible features of the printed surface, particularly the layer lines—horizontal ridges created during the layer-by-layer deposition process in 3D printers. Each of these molds had different surface textures, which made it important to understand how their surface structure affected light transmission to the solar cell once the micro-pod was formed. As light passes through the encapsulation, the surface structure can cause it to either reflect, scatter or transmit more directly. This behaviour significantly impacts how efficiently the light reaches the solar cell. With the mold cast from the PLA, for example, the thick printing lines disrupted the light path, causing increased reflection and less efficient light transmission. For the mold cast from the PVA, which is a soft and biodegradable polymer that is highly sensitive to moisture, it was envisioned that the printed edges and corners could be dissolved with water, to achieve a smoother, non-textured surface that would allow light to pass more effectively. However, due to the small size of the encapsulation (~3 mm), controlling the dissolution process was difficult, leading to inconsistent results and a surface that still was not smooth. The SLA printing with 20K resin produced high-resolution, finely detailed prints with smooth surface finishes compared to the PLA, and PVA. It created a final mold with a smoother surface that reduced light reflection and allowed for better light transmission to the solar cell. Examples of encapsulated solar cells created using the different mold types are shown in Fig. 8.

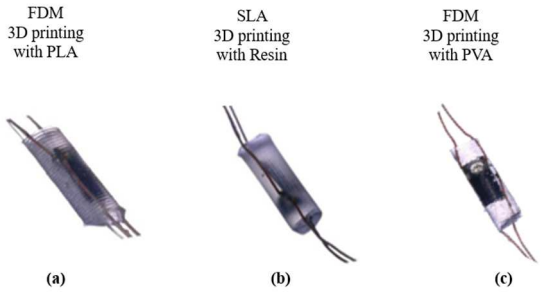


Fig. 8. Solar cells encapsulated in resin micro-pods formed using single-part molds created using different 3D printed master molds with different surface structures (a) FDM printing with PLA, larger layer lines. (b) SLA printing with 20K resin, finer layer lines. (c) FDM printing by PVA, non-uniform surface.

A comparison of the I-V curves for a single encapsulated solar cell created with each mold (shown in Fig. 9) indicated the mold created from the resin master-mold was the superior option with $I_{sc}$ 3.56 mA compare to PLA and PVA with 3.42 and 3.29 mA respectively. Therefore, the resin emerged as a more favorable option in terms of final shape, surface structure, electrical characteristics ($V_{oc}$, and $I_{sc}$). The better electrical response for large-scale production with more solar cells embedded in the yarn made the resin better option to choose.

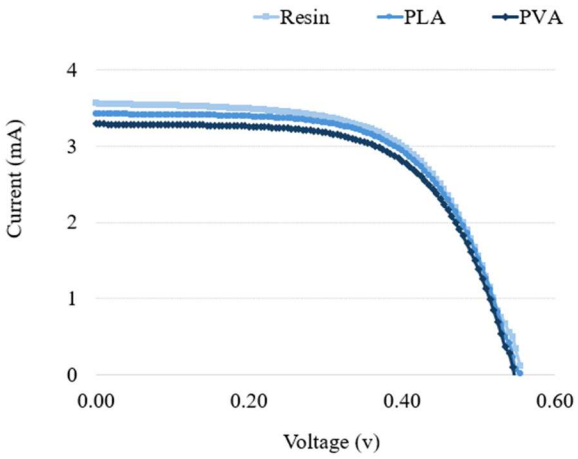


Fig. 9. I-V curves for solar cells encapsulated in resin micro-pods formed using single-part molds created using different 3D printed master molds.

*B. Developing and testing a knitted structure for embedding solar electronic yarns*

The initial trial textile sample is shown in Fig. 10. In this sample, three channels with varying coverage (without coverage, half coverage, and almost covered) were created at the base of the knitted polyester swatch to allow for the insertion of the solar E-yarn into the fabric. To achieve this, in the section labeled "a", an eyelet was created in the channel after determining the solar cell's placement. This opening allowed the surface of the solar E-yarn to remain exposed. In other words, a hole in part of the channel was made to uncover the surface of the solar E-yarn. The downside of this design was that, although the fabric allowed sunlight to pass through as it was not blocking the surface of the solar cell it still did not meet the aesthetic criteria for textile design. Careful design of the placement and positioning of the solar cells was also crucial, as even a slight misalignment could change their positions, especially for E-yarns with multiple embedded solar cells. The eyelet in the channel made it difficult to insert the solar E-yarn, which affected the braiding coverage as it passed through the channels. To solve this issue, the channels labeled b and c were added. However, even with these changes, the surface of the solar cell was still partially and nearly fully covered by the channels. This necessitated precise positioning of the solar cell in a specific area, making the design impractical for real-world applications.

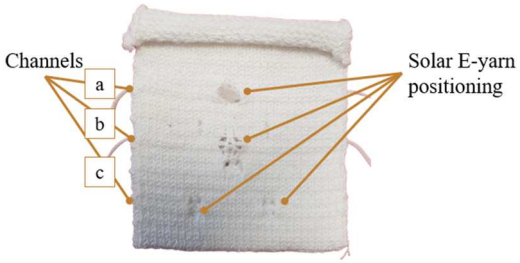


Fig. 10. Sample knitted E-textile with three knitted channels, (a) non-covered, (b) partially covered, (c) fully covered.

In the next design, a less dense channel that spanned the entire area was created, rather than making an eyelet through the channel. This modification allowed for greater flexibility in positioning the solar E-yarn, eliminating the restriction of having to place it in a specific spot. Additionally, a different material for the channel was explored, as polyester had been obstructing the surface of the solar E-yarn. A swatch with a 50 × 50 mm active area was created using transparent filaments for the channels. This swatch was deformable, as shown in Fig. 11.

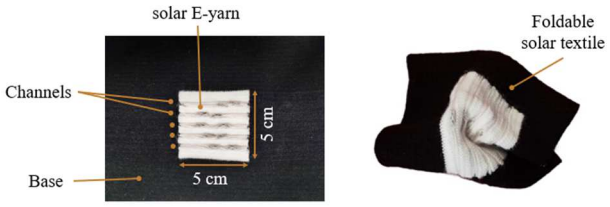


Fig. 11. Improved knitted solar textile sample. The body and base are made of polyester, and the channels are transparent filaments.

The swatch was tested under 1 Sun to evaluate its performance (Fig. 12). The results showed a short-circuit current ($I_{sc}$) of 18.17 mA, an open-circuit voltage ($V_{oc}$) of 0.52 V, and a maximum power output of 9.5 mW.

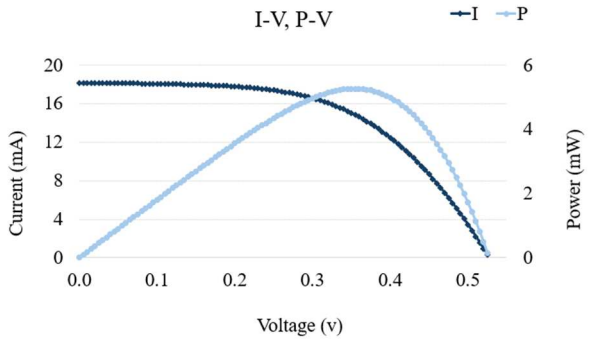


Fig. 12. Current-voltage (I-V) and power-voltage (P-V) characteristics of a 50×50 mm knitted swatch. The swatch contains five polycrystalline solar E-yarns connected in parallel, with each channel featuring two parallel solar cells.

One concern with using the straight channel, especially for wearable applications was the limited stretchability of the structure, which is crucial for garments that need to accommodate movement. Further, there was an increased risk of wire disconnection when the fabric was stretched. To address this, designs for integrating solar E-yarns into textiles where stretch could be achieved in two dimensions were explored. One promising solution we discovered was the wavy pattern, and the progress in creating this type of design is shown in Fig. 13.

Fig. 13. Progress in developing a wavy pattern design for integrating solar E-yarns into textiles.

Compared to using straight channels, the wavy pattern offered several advantages. Firstly, it allowed for more solar cells to be incorporated into the same length of fabric, increasing the potential power generation. Secondly, the wavy arrangement provided greater flexibility and stretchability for the E-yarns when embedded into the fabric (the key reason that this design was explored). This flexibility enhanced the yarn's ability to move and stretch with the fabric, making it more suitable for wearable applications where comfort and durability are key. Taking these factors into account, a swatch featuring a more flexible and stretchable structure to enhance both functionality and durability for wearable use was created, as shown in Fig. 14.

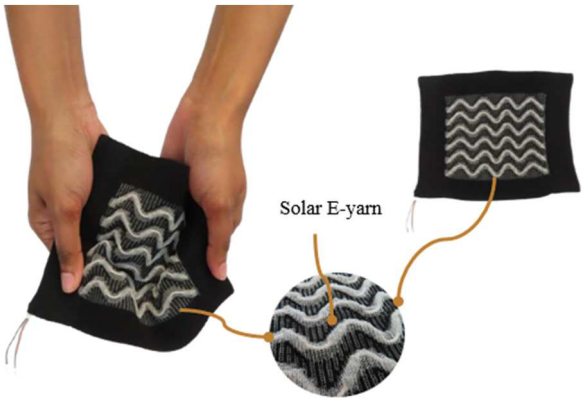


Fig. 14. The knitted solar textile. A wavy structure was used to incorporate the E-yarns allowing for a stretch in two dimensions. The panel was 180×140 mm, with an active area of 100×100 mm, a channel width of 5mm, gaps between the channels 10 mm, and contained 48 solar cells. The body and base of the material were black polyester, and the channels were made from transparent filaments.

### *C. Evaluating the knitted solar textiles' performance*

The knitted solar textile was tested outdoors under varying light intensities to assess its performance. The specification for each solar E-yarn with a single solar cell was an average short-circuit current (Isc) of 1.3 mA and an open-circuit voltage (Voc) of 0.56 V. Based on these values, the expected power output for the solar E-yarns, when not integrated into the fabric, was expected to be 62.4 mW under 1 Sun illumination.

The maximum output power obtained from the outdoor tests averaged 53 mW, indicating that this configuration achieved approximately 84.9% of the expected power output. It is important to note that embedding solar E-yarns into the fabric would likely reduce the power output due to the absorption and scattering of light by the fabric material (Fig. 15).

Data collected for the solar textile under different lighting conditions is shown in Table 2.

TABLE II. RESULTS FROM TESTING THE KNITTED SOLAR TEXTILE OUTSIDE UNDER DIFFERENT LIGHTING CONDITIONS.

| **Irradiance: $G_1$ (W/m²)** | **V (v)** | **I (mA)** | **$P_1$ (mW)** | **$P_2$ (mW) for 1 Sun** |
|---|---|---|---|---|
| 557 | 1.076 | 28.40 | 30.56 | 54.86 |
| 545 | 1.069 | 27.88 | 29.80 | 54.69 |
| 533 | 1.061 | 26.68 | 28.31 | 53.11 |
| 504 | 1.053 | 25.50 | 26.85 | 53.28 |

$$P_2 = P_1 \times (G_2/G_1) \quad (1)$$

where $P_2$ the power for 1 Sun is calculated by Equation 1, and $G_2$ irradiance for 1 Sun is 1000 (W/m$^2$) [35].

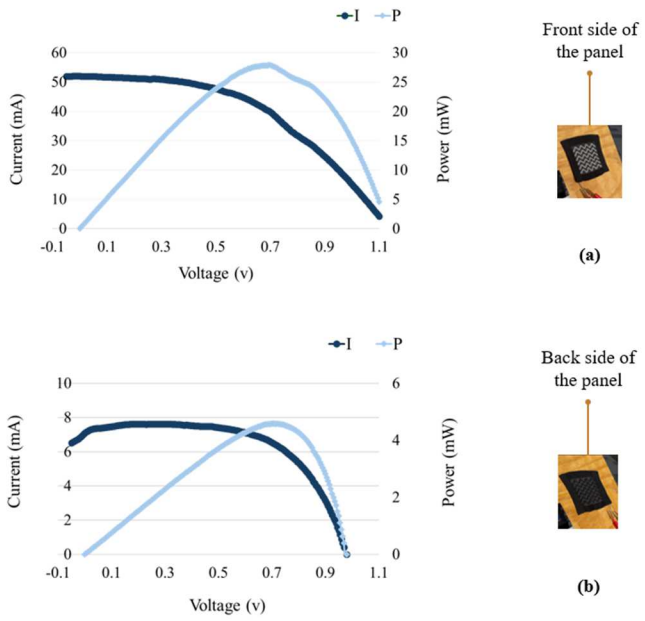


Fig. 15. I-V and P-V curves of the a. front and b. back sides of the knitted solar textile during outdoor testing.

### *D. Textile property testing of the knitted solar textile*

Air permeability measurements were conducted before and after incorporating solar E-yarns into the swatch. A microscope image compares the fabric structure and the results are shown in Fig. 16.

The air permeability before insertion was low at 195 ± 0.5 mm/s; after insertion, it increased to 716 ± 2.65 mm/s. It is believed that the insertion of solar E-yarns to some extent caused the knitted structure to relax, leading to a more porous structure and allowing more air to pass through.

For the tensile test, the swatch was positioned between grips with a length grip-to-grip separation of 132 mm in the course direction, stretching it to a desired strain percentage of 25 %. The strain percentage was calculated using the following Equation 2:

$$\text{Strain (\%)} = 100 \times (L_1 - L_0) / L_0 \quad (2)$$

$L_1$ is the final length, and $L_0$ is the initial length. So, the strain was measured at 25%, with a maximum force of 9.183 N, resulting in a current drop of 34% in the most stretched position.

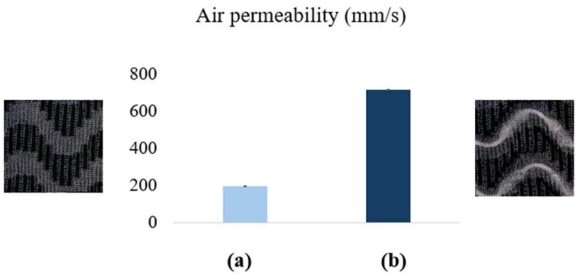


Fig. 16. Air permeability and microscope image comparing the fabric structure a. before and b. after the insertion of solar E-yarns.

For the vertical orientation (wale direction) the grip-to-grip length (the initial length), in the course direction, was 108 mm, the strain percentage was 11.92 %, and the required force

to reach the desired strain percentage was 15 N. A drop in current by 26% was observed.

The results showed that this knitted solar textile configuration offers stretchability in both directions, with distinct behaviours based on the stretch direction. In the course direction, the textile is more stretchable, extending by 25 % under a moderate force of 9 N. Conversely, in the wale direction, the material is less stretchable at 12 % but more rigid, requiring a higher force of 15 N. This combination of stretchiness in one direction and strength in the other makes it a good fit for flexible electronics (Fig. 17).

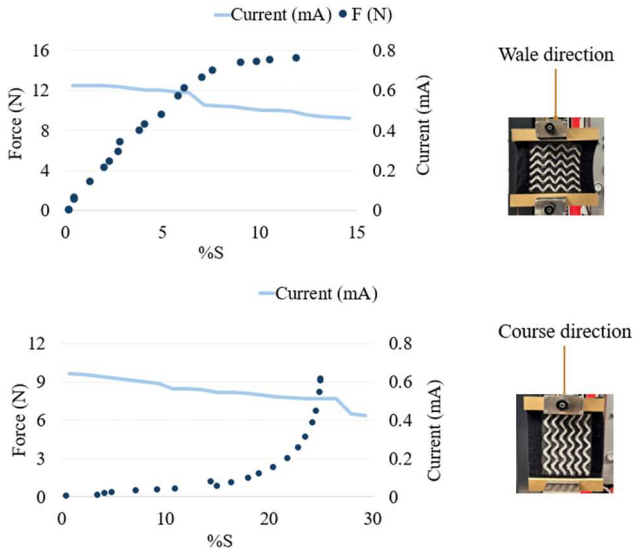


Fig. 17. Comparison of stretchability in the course and wale directions of the knitted solar textile.

## IV. Conclusion

In conclusion, this study developed and evaluated a novel knitted solar textile system that effectively integrates solar electronic yarns within a flexible, stretchable, and breathable fabric structure. While most solar textiles rely on woven base fabrics or conductive woven elements for stability and electrical function, utilizing a knitted structure presents superior benefits such as enhanced porosity and stretchability, which are challenging to achieve with woven materials. It also simplifies maintenance and error identification, enabling quick and easy replacement of solar E-yarns. While in the woven structure, in contrast, replacing electronics poses significant challenges, often requiring the entire setup to be unraveled, which can be highly time-consuming and cumbersome.

Although some research has explored knitted textiles as coverings for solar cells [36], fully integrated knitted solar textiles remain largely unexplored. This work represents an advancement in solar textile design by introducing a porous, flexible, and stretchable fabric structure that integrates solar functionality. This approach could support the development of wearable and adaptable solar applications.

This study builds on previous in-depth research into the key stages of solar textiles production using E-yarn technology and focuses on the design and optimization of the structure and material for the encapsulation step as well as the fabric structure. The work aimed to refine encapsulation techniques to improve light transmission, stability, and durability of the solar cells embedded in the yarn. Also, an optimized knitted structure was developed featuring a wavy channel pattern, which is more reliable, durable, and sustainable compared to the other embedding techniques. This innovative design improves flexibility and mechanical stretchability, enabling a greater density of solar cells to be embedded into the fabric. It also supports efficient replacement and fault recognition, which solar E-yarns can be swapped out without extensive downtime or complex processes, which are critical for integrating reliable solar electronic functionality into fabric-based applications.

With these improvements, a knitted foldable, stretchable solar textile measuring an active area of 100×100 mm was produced which displayed promising electric and textile performance: Achieving approximately 55 mW power output under real-world outdoor testing conditions. Besides the electrical improvement, through this configuration, the textile property assessments of the panel demonstrated that the design preserves essential qualities such as air permeability and tensile strength in both horizontal and vertical directions, enhancing comfort and durability if applied to wearables.

Overall, this work advances the potential for scalable, energy-harvesting textile systems by offering a durable, lightweight, and modular approach that balances both aesthetic and functional requirements.

Future studies should focus on optimising fabric architecture further for multi-axis stretchability and assessing long-term durability under varied environmental conditions to fully realize the potential of solar-integrated textiles in sustainable, wearable technology applications.

## Acknowledgments

This research was funded by the Engineering and Physical Sciences Research Council (EPSRC) grant EP/T001313/1 Production engineering research for the manufacture of novel electronically functional yarns for multifunctional smart textiles.

The authors would like to thank Nottingham Trent University, (United Kingdom) for providing Parvin with a studentship to conduct this research. The authors would like to specifically thank the Nottingham School of Art & Design for providing other financial support to enable this research. The authors would also like to thank Richard Arm, Andreea Pislaru, Russell Metcalfe, and Kalana Marasinghe for their technical support.

Data are contained within the article. The raw datasets collected for the analysis of this study can be found on figshare at 10.6084/m9.figshare.27382104.

## References

[1] M. Gao et al., “Power generation for wearable systems,” Apr. 01, 2021, Royal Society of Chemistry. doi: 10.1039/d0ee03911j.

[2] G. Aroganam, N. Manivannan, and D. Harrison, “Review on Wearable Technology Sensors Used in Consumer Sport Applications,” Aug. 2021. doi: 10.3390/s19091983.

[3] M. Liu, F. Qian, J. Mi, and L. Zuo, “Biomechanical energy harvesting for wearable and mobile devices: State-of-the-art and future directions,” Appl Energy, vol. 321, Sep. 2022, doi: 10.1016/j.apenergy.2022.119379.

[4] K. Hinde, G. White, and N. Armstrong, “Wearable devices suitable for monitoring twenty four hour heart rate variability in military populations,” Feb. 02, 2021, MDPI AG. doi: 10.3390/s21041061.

[5] Ramdayal and K. Balasubramanian, “Advancement in textile technology for defence application,” 2013, Defense Scientific Information and Documentation Centre. doi: 10.14429/dsj.63.2756.

[6] H. Liu et al., “A promising material for human-friendly functional wearable electronics,” Feb. 01, 2017, Elsevier Ltd. doi: 10.1016/j.mser.2017.01.001.

[7] A. Ometov et al., “A Survey on Wearable Technology: History, State-of-the-Art and Current Challenges,” Jul. 05, 2021, Elsevier B.V. doi: 10.1016/j.comnet.2021.108074.

[8] C. W. Kan and Y. L. Lam, “Future trend in wearable electronics in the textile industry,” 2021, MDPI AG. doi: 10.3390/app11093914.

[9] D. Gharode, A. Nella, and M. Rajagopal, “State-of-art design aspects of wearable, mobile, and flexible antennas for modern communication wireless systems,” International Journal of Communication Systems, vol. 34, no. 15, Oct. 2021, doi: 10.1002/dac.4934.

[10] V. Bhatnagar and P. Owende, “Energy harvesting for assistive and mobile applications,” May 01, 2015, John Wiley and Sons Ltd. doi: 10.1002/ese3.63.

[11] Y. W. Chong, W. Ismail, K. Ko, and C. Y. Lee, “Energy Harvesting for Wearable Devices: A Review,” IEEE Sens J, vol. 19, no. 20, pp. 9047–9062, Oct. 2019, doi: 10.1109/JSEN.2019.2925638.

[12] F. Yildiz, “Potential Ambient Energy-Harvesting Sources and Techniques,” The Journal of Technology Studies, 2009.

[13] M. Magno and D. Boyle, “Wearable Energy Harvesting: From body to battery,” in Proceedings - 2017 12th IEEE International Conference on Design and Technology of Integrated Systems in Nanoscale Era, DTIS 2017, Institute of Electrical and Electronics Engineers Inc., May 2017. doi: 10.1109/DTIS.2017.7930169.

[14] M. Takamiya, “Energy efficient design and energy harvesting for energy autonomous systems,” in 2015 International Symposium on VLSI Design, Automation and Test, VLSI-DAT 2015, Institute of Electrical and Electronics Engineers Inc., May 2015. doi: 10.1109/VLSI-DAT.2015.7114542.

[15] T. J. Kazmierski and S. Beeby, “Energy Harvesting Systems: Principles, Modeling and Applications,” Nano Energy, 2011.

[16] B. Han et al., “Harvesting energy from vibrations of the underlying structure,” JVC/Journal of Vibration and Control, vol. 19, no. 15, pp. 2255–2269, Nov. 2013, doi: 10.1177/1077546313501537.

[17] B. Dziadak, Ł. Makowski, and A. Michalski, “Survey of energy harvesting systems for wireless sensor networks in environmental monitoring,” Metrology and Measurement Systems, vol. 23, no. 4, pp. 495–512, 2016, doi: 10.1515/mms-2016-0053.

[18] M. Ghahremani Honarvar and M. Latifi, “Overview of wearable electronics and smart textiles,” Apr. 03, 2017, Taylor and Francis Ltd. doi: 10.1080/00405000.2016.1177870.

[19] C. Dang et al., “Fibres-threads of intelligence-enable a new generation of wearable systems,” Aug. 01, 2024, Royal Society of Chemistry. doi: 10.1039/d4cs00286e.

[20] M. B. Schubert and J. H. Werner, “Flexible solar cells for clothing,” 2006.

[21] A. S. Satharasinghe, “Development of Solar Energy Harvesting Textile,” 2019.

[22] A. Satharasinghe, T. Hughes-Riley, and T. Dias, “A Review of Solar Energy Harvesting Electronic Textiles,” Sensors (Basel), vol. 20, no. 20, pp. 1–39, Oct. 2020, doi: 10.3390/S20205938.

[23] Z. Abdin et al., “Solar energy harvesting with the application of nanotechnology,” 2013. doi: 10.1016/j.rser.2013.06.023.

[24] V. Raghunathan, A. Kansal, J. Hsu, J. Friedman, and M. Srivastava, “Design considerations for solar energy harvesting wireless embedded systems,” in 2005 4th International Symposium on Information Processing in Sensor Networks, IPSN 2005, 2005, pp. 457–462. doi: 10.1109/IPSN.2005.1440973.

[25] L. Xu et al., “A perovskite solar cell textile that works at-40 to 160 °c,” J Mater Chem A Mater, vol. 8, no. 11, pp. 5476–5483, Mar. 2020, doi: 10.1039/c9ta13785h.

[26] S. Arumugam et al., “Fully spray-coated organic solar cells on woven polyester cotton fabrics for wearable energy harvesting applications.” Accessed: May 18, 2023. [Online]. Available: https://pubs.rsc.org/en/content/articlelanding/2016/ta/c5ta03389f/unauth

[27] T. Dias and A. Ratnayake, “Integration of micro-electronics with yarns for smart textiles,” in Electronic Textiles: Smart Fabrics and Wearable Technology, Elsevier Ltd, 2015, pp. 109–116. doi: 10.1016/B978-0-08-100201-8.00006-0.

[28] A. A. Simegnaw, B. Malengier, G. Rotich, M. G. Tadesse, and L. Van Langenhove, “Review on the integration of microelectronics for e-textile,” Sep. 01, 2021, MDPI. doi: 10.3390/ma14175113.

[29] A. Komolafe et al., “E-Textile Technology Review-From Materials to Application,” IEEE Access, vol. 9, pp. 97152–97179, 2021, doi: 10.1109/ACCESS.2021.3094303.

[30] H. Liu et al., “Paper: A promising material for human-friendly functional wearable electronics,” Feb. 01, 2017, Elsevier Ltd. doi: 10.1016/j.mser.2017.01.001.

[31] N. Abeywickrama et al., “The Design and Development of Woven Textile Solar Panels,” Materials, vol. 16, no. 11, Jun. 2023, doi: 10.3390/ma16114129.

[32] Parvin Ebrahimi et al., “Characterization and Optimization of Solar Energy Harvesting Textile to Power Wearable Devices,” E-Textile Conference 2023., 2023.

[33] A. S. Satharasinghe, T. Hughes-Riley, T. Dias, and A. Satharasinghe, “WEARABLE AND WASHABLE PHOTOVOLTAIC FABRICS,” 2019, doi: 10.4229/EUPVSEC20192019-1BO.9.2.

[34] A. M. Shahidi et al., “Quantification of Fundamental Textile Properties of Electronic Textiles Fabricated Using Different Techniques,” Textiles, vol. 4, no. 2, pp. 218–236, Jun. 2024, doi: 10.3390/textiles4020013.

[35] Mertens Konrad, “Photovoltaics: Fundamentals, Technology and Practice,” Wiley, 2018.

[36] F. Elsehrawy, B. Blomstedt, E. Ilén, E. Palovuori, and J. Halme, “Optimisation of knitted fabrics as visually concealing covers for textile-integrated photovoltaics,” Solar Energy Materials and Solar Cells, vol. 252, Apr. 2023, doi: 10.1016/j.solmat.2023.112205.